Report on visibility tests with ALARO on cycle 43 t2 bf10 at SHMÚ

André Simon, Martin Dian

SHMÚ

Technical part:

The visibility parameter was originally coded at Meteo France by Ingrid Etchevers (Dombrowski-Etchevers et al., 2018) for the AROME model and later implemented and tested in ALARO at CHMI (by Radmila Brožková) and at ARSO (by Piotr Sekula). The original code was modified at CHMI for the ALARO model, a new routine (phys_dmn/acvisih.F90) has been created to calculate visibility. Output parameters (PVISICLD, PVISIHYD) are visibility with respect to cloud liquid water (fog) and visibility concerning precipitation, which units are meters. Another product (PMXCLWC) is related to cloud liquid water content (kg/kg) and it was created for verification purposes. The outputs refer to the height HVISI above the terrain, which cannot be lower than the lowest vertical level (KLEV). The minimum visibility and maximum of cloud liquid water content is determined for a chosen period, which is set as parameters NVISIPERIOD (default 3600s) or NVISIPERIOD2 (900s) in NAMXFU. The maximum value of visibility is limited to 20 km. The direct inputs are hydrometeors (cloud liquid and solid water, rain, snow and graupel) and their mixing ratios, multiplied by air density (original units for hydrometeors are kg/kg but g/m^3 is used in visibility formulas).

The routines, which were modified with respect to the reference were:
adiab/cpg_dia.F90 adiab/cpg.F90
control/cnt4.F90
dia/cpxfu.F90
fullpos/fpcorphy.F90 fullpos/hpos_xfu.F90 fullpos/sufpxfu.F90
module/ptrxfu.F90 module/yomafn.F90 module/yomphy2.F90 module/yomxfu.F90
namelist/namafn.nam.h namelist/namphy2.nam.h namelist/namxfu.nam.h
phys_dmn/acvisih.F90 phys_dmn/aplpar.F90 phys_dmn/initaplpar.F90
phys_dmn/mf_phys.F90 phys_dmn/suphy2.F90
setup/suafn1.F90 setup/suafn2.F90 setup/suafn3.F90 setup/suxfu.F90

At SHMU, some minor additional changes in the local pack cy43t2bf10v01 were done, mainly some cleaning of code not related to visibility. The operational pack at the SHMU computer containing visibility is: /data/users/nwp002/pack/43t2_bf10_export.05.oper.01.MPIGNU493.x

The hydrometeors must be included in order to calculate visibility. First, e001 had to be run (on SHMU domain, 63 vertical levels, 4.5 km horizontal resolution) and the namelist for e001 included:

NAMAFN:
GFP_VISICLD%IBITS=12,
GFP_VISIHYD%IBITS=12,
GFP_MXCLWC%IBITS=12,

NAMXFU:
LXVISI=.TRUE., (activates the visibility diagnostics)

In order to write hydrometeors to output icmsh file, the following variables must be switched in NAMGFL, e.g. for the cloud liquid water: YL_NL%LGP=.TRUE., YL_NL%NREQIN=1, YL_NL%LREQOUT=.TRUE.,

This setting provides the above mentioned three parameters as outputs in historical files (CLS.VISICLD, CLS.VISIPRE, MAXCLWC). These were related solely to the NVISIPERIOD (3600s). However, it would be possible to calculate simultaneously additional visibility parameters (CLS.VISICLD2, CLS.VISIPRE2, MAXCLWC2) for the 15 min. or shorter period, which is better for the evaluation of visibility related to convective precipitation.

The link to the e001 namelist at the SHMU computer is: /users/nwp109/wrk/nam/cy43t2/vis2/e001_ALARO-1_CY43T2bf09_vis2tke.nam

It is also possible to make full-pos for the visibility parameters. Besides visibility parameters we postprocessed the fields of respective hydrometeors and the simulated radar reflectivity. This required changes of the original namelist in NAMAFN (e.g. TFP_L%CLNAME='LIQUID_WATER', TFP_L%LLGP=.T., while TFP_SRE%LLGP=.F.), in NAMGFL (e.g. YL_NL%LGP=.TRUE., YL_NL%LSP=.FALSE., YL_NL%NREQIN=1,) and addition of parameters in NAMFPC (e.g. CFP3DF(6)='SIM_REFLECTI', CFPXFU(9)='CLS.VISICLD', CFPXFU(10)='CLS.VISIPRE'). There was no reference full-pos namelist for cy43t2, so it was adapted from cycle 40.

The link to the full-pos namelist at the SHMU computer is: /users/nwp109/wrk/nam/cy43t2/vis2/fp_CY43T2bf09_vis2_spectr.nam

The relationship between the hydrometeors and visibility can be modified with various parameters. For the presented first tests we used the basic (default) setup including parameters:

NAMPHY2:
HVISI=5m
COEFFEXTQ(1)=16.14
COEFFEXTQ(2)= 163.9
COEFFEXTQ(3)= 2.5
COEFFEXTQ(4)= 10.4
COEFFEXTQ(5)= 2.4
COEFFEXTQ(6)= 2.4

COEFFPWRQ(1)=0.27
COEFFPWRQ(2)=1
COEFFPWRQ(3)= 0.75
COEFFPWRQ(4)= 0.78
COEFFPWRQ(5)= 0.78
COEFFPWRQ(6)= 0.78

The formula for visibility calculation (using Koschmieder's law) yields:

$$PVISICLD = z_s\, z_c\, \{\beta_0 + \beta_{lwc} + \beta_{ice}\}^{-1}, \qquad (1)$$

where
$Zs = z_{scale} = 1000$, $Zc = z_{contrast} = -\ln(0.05)$, $\beta_0 = \beta_{Rayl} = 0.013$

The extinction coefficients of cloud liquid water (*lwc*) and ice are as follows (after Kunkel, 1984):

$$\beta_{lwc} = C_{EQ1}\,(z_s\,\rho\,q_{lwc})^{C_{PQ1}}\,,\ \beta_{ice} = C_{EQ2}\,(z_s\,\rho\,q_{ice})^{C_{PQ2}}$$

Where q_{lwc} , q_{ice} is the cloud liquid (ice) water content in kg/kg, respectively, ρ is air density in kg m^{-3}. The use of density and z_{scale} parameter is due to conversion of the water (ice) content from kg/kg to g m^{-3} units. It is important to note that the model visibility calculation currently uses a cloud liquid water product derived for the radiation scheme (PQLI in APLPAR). Compared to standard diagnostic cloud liquid water (PQL or ZQL in APLPAR) this product is more complex and more consistent concerning physical processes in clouds, exhibits only positive values, etc. On the other hand, PQLI attains significant values only in clouds, which means that visibility is set to its maximum and it is rather uniform outside of the clouds.
The coefficients C_{EQ1} , C_{PQ1} are the COEFFEXTQ(1), COEFFPWRQ (1) for cloud liquid water. The parameters COEFFEXTQ(2), COEFFPWRQ (2) denote coefficients for cloud ice water content.

The visibility related to precipitation (rain, snow, graupel) is defined in similar manner as for the cloud liquid water:

$$PVISIHYD = z_s\, z_c\, \{\beta_0 + \beta_{rain} + \beta_{snow} + \beta_{graupel}\}^{-1}, \quad (2)$$

where $\beta_{rain} = C_{EQ3}\,(z_s\,\rho\,q_{rain})^{C_{PQ3}}$, $\beta_{snow} = C_{EQ4}\,(z_{scale}\,\rho\,q_{snow})^{C_{PQ4}}$,
$\beta_{graupel} = C_{EQ5}\,(z_s\,\rho\,q_{graupel})^{C_{PQ5}}$

The respective coefficients C_{EQi} , C_{PQi} are the COEFFEXTQ(i), COEFFPWRQ (i) parameters, where the index "i" is 3 for rain, 4 for snow and 5 for graupel. Graupel mixing ratio was not available for these tests.

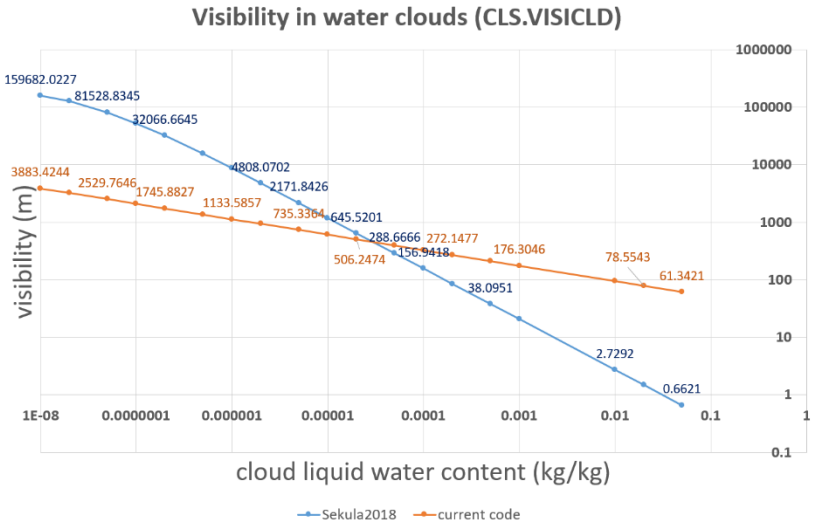

Figure1: Visibility (m) as function of cloud liquid water (kg/kg) only ($\beta_{ice} = 0$) as described in the report of Sekula (2018) in blue color and as defined in the current code default settings (Philip, 2016), used in the presented tests (orange). Both axes use logarithmic scale. Some visibility records are emphasized by numbers.

The default setting of COEFFEXTQ(1) and COEFFPWRQ (1) for cloud liquid water was obtained from visibility observations in France (Philip, 2016). A different setting was tested by Sekula (2018) in his CASE1, where COEFFEXTQ(1) would yield 144.7 and COEFFPWRQ(1)=0.88 for the cloud liquid water (inspired by the research of Stoelinga, 1999). The two settings give significantly different results for visibility in water clouds, above all in case of low cloud liquid water mixing ratios (see Figure1). One can see that with the default setting the visibility would practically never exceed 4 km, while in the setting of Sekula-CASE1 the visibility would rise much more rapidly with decreasing cloud liquid water content, which is more realistic.

Besides formulas, where visibility in clouds is solely function of the liquid/ice water content, there exist relationships derived upon measurements with spectrometers and field experiments showing dependency on both q_{lwc} , q_{ice} and on the droplet/crystal number concentration (Gultepe, 2006, Gultepe, 2007, Gultepe, 2010).

$$VIS = k \left(\frac{1}{q_{lwc} N_d}\right)^m, \quad (3)$$

where *k* and *m* are coefficients similar to C_{EQi} , C_{PQi} .

Such relationships are probably more accurate, although for example the droplet number concentration (Nd) in fog also depends on q_{lwc}. Observations (Gultepe, 2006) indicate that such function is probably quadratic:

$$q_{lwc} = 1\ 10^{-6}\ N_d^2 + 0.0014\ N_d \quad (4)$$

This can be used to emulate visibility parameterization also in case, one knows only q_{lwc} (N_d is available in the ECMWF physics as parameter ZDNC in aer_diag1.F90 and it will be available also in the LIMA scheme in AROME). It is also possible to linearize such VIS and q_{lwc} relationship to a great extent and find such setting of C_{EQ1} , C_{PQ1} , which nearly describes the original VIS(q_{lwc} , N_d) equation (3). We evaluated three main settings of "k" and "m" corresponding to findings of fog research (Gultepe, 2006, Gultepe, 2007, Gultepe, 2010).

Parameterization	k	m	C_{EXTQ1}	C_{PWRQ1}
Gultepe 2006	1.002	0.6473	202.8162	1.3233
Gultepe 2007 (used also in Monte et al., 2017)	1.13	0.51	72.8498	1.0358
Gultepe, 2010	0.87706	0.49034	80.9636	0.9851

Table 1: Various settings of parameters "k" and "m" for the cloud visibility VIS(q_{lwc} , N_d) formula (3) presented in studies of Gultepe. The 4th and 5th column shows the best fit of ALARO parameterization when modifying C_{EQ1} and C_{PQ1}.

In comparison with current code defaults and tests of Sekula (CASE1), the approaches based on Table 1 and equation (3), (4) show a substantially different behaviour, although the representation of visibility with respect to q_{lwc} is relatively close by liquid water content about 1 10^{-5} - 1 10^{-4} kg/kg (Fig. 2). The main difference is that settings described by articles of Gultepe predict steeper increase of visibility in regions with low q_{lwc}. For some settings (Gultepe 2006), one can also obtain lower visibility in regions with high liquid water content.

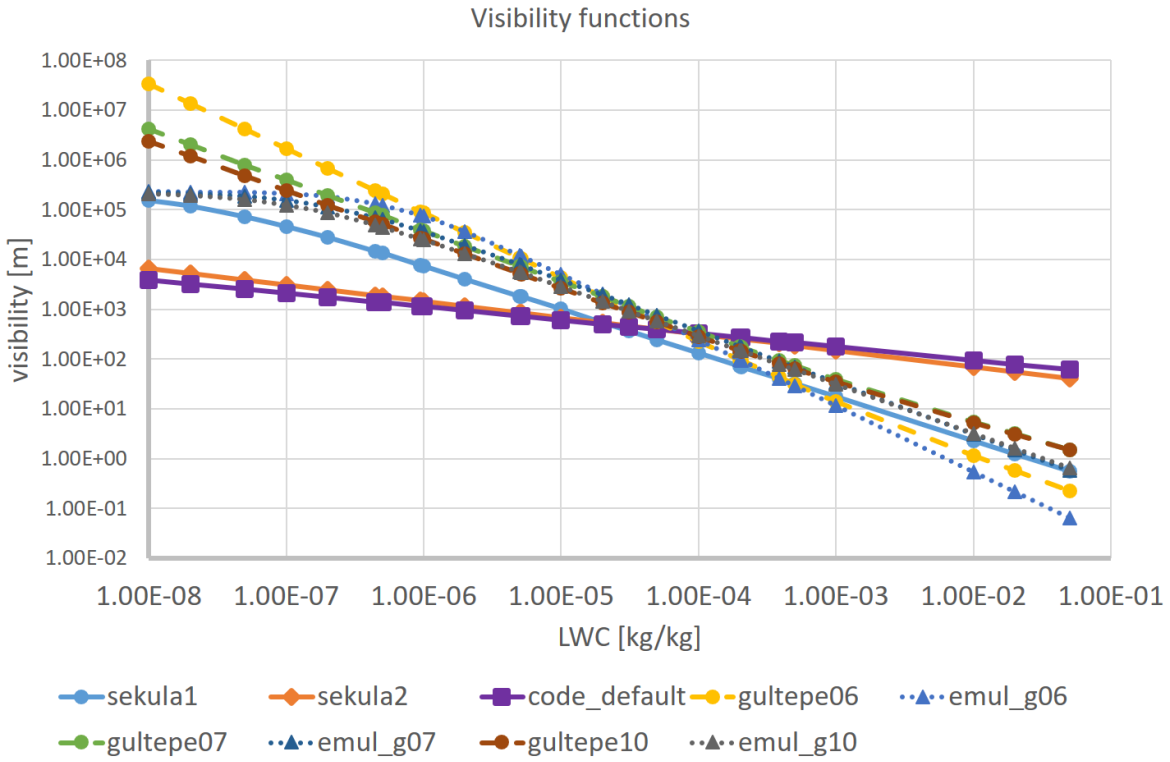

Fig. 2 Visibility (m) as function of cloud liquid water (kg/kg) only ($\beta_{ice} = 0$) as described in the report of Sekula (2018) – sekula 1 (his CASE1) and sekula 2(his CASE2), as defined in the current ALARO code default settings of C_{EQ1} and C_{PQ1} (code_default) and as defined in various studies of Gultepe (see Table 1). The abbreviations emul_g06, emul_g07, emul_g10 show courses of the visibility function obtained with ALARO parameterisation emulating the Gultepe (2006), Gultepe (2007) and Gultepe (2010) relationships based on the Eq. (4). The scales are logarithmic.

Results:

Case1: Comparison with AROME

Both visibility parameters were tested on three cases. The first one was the 06 January 2019 situation already tested at Meteo France on AROME (Piriou et al., 2019):

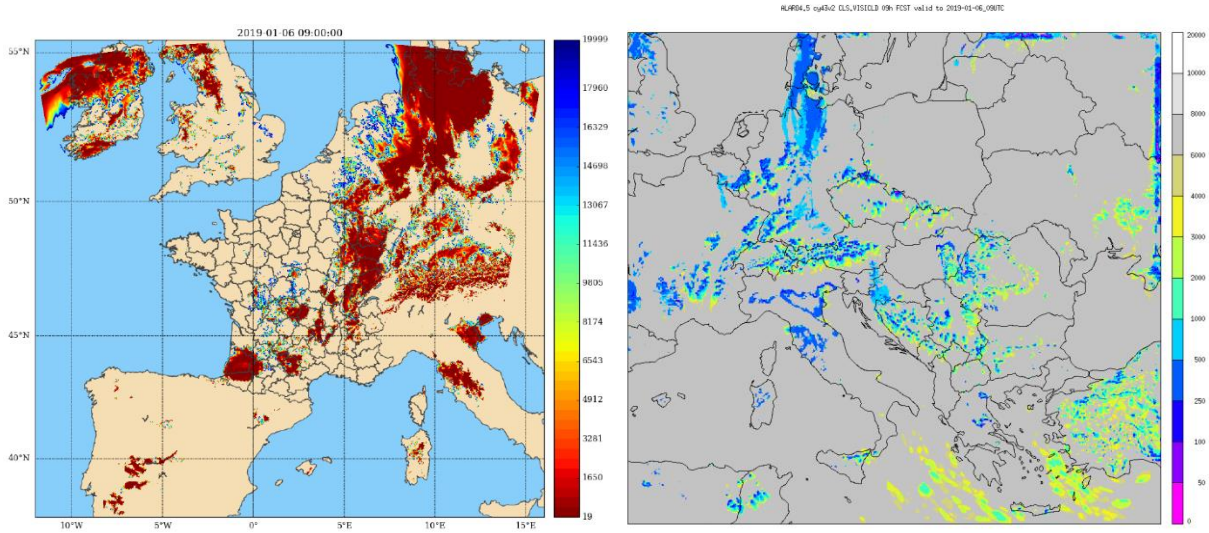

Fig. 3a: Left: 9h forecast of visibility (m) from the AROME model valid to 06 January 2019 09 UTC (Piriou et al., 2019). Fig. 3b: Right: Forecast of 1h minimum visibility in clouds (CLS.VISICLD) from ALARO SHMU cy43t2 for the same date and time with default setting. Conditions for fog (visibility < 1km) are in bluish colors.

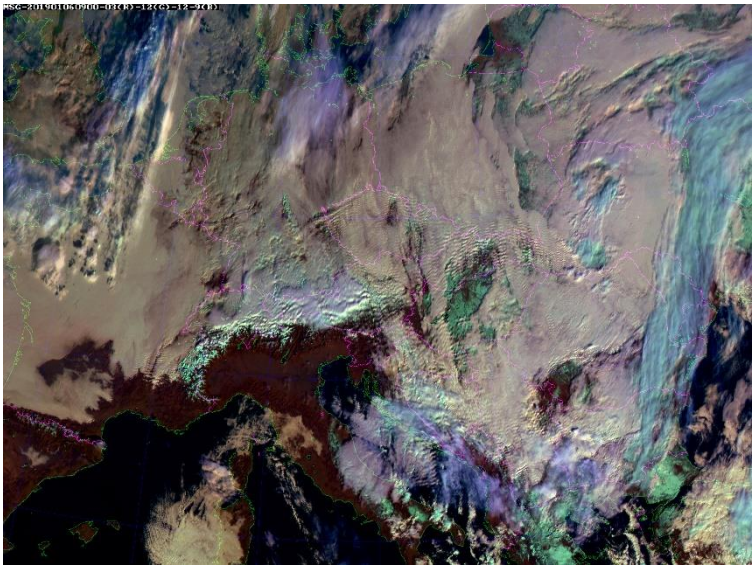

Fig. 4: Meteosat 8 (MSG) Natural color RGB image valid to 06 January 2019 09 UTC.

The comparison with ALARO results (Fig. 3) shows that fog (visibility below 1km) occurred in several areas, where it was forecast by AROME as well. This concerns a compact, large area of northern Germany. Very low visibility was predicted for mountain area of Czech Republic (Krkonoše, Jizerské hory) or Alps. Fog was predicted for the southwestern part of Tuscany and for the Po valley (Italy). In ALARO there is a non-realistic artefact in the latter region. Comparison with satellite imagery (Fig. 4) shows that there was no fog in the Po valley but some areas in Tuscany could be overlaid by fog or low-level clouds at that time. The satellite image also shows large areas of low-based cloudiness or

fog over France, though, in ALARO, these were rather isolated territories. It is difficult to evaluate the presence of fog over Germany or Alps solely upon satellites because there were medium- and high-based clouds too.

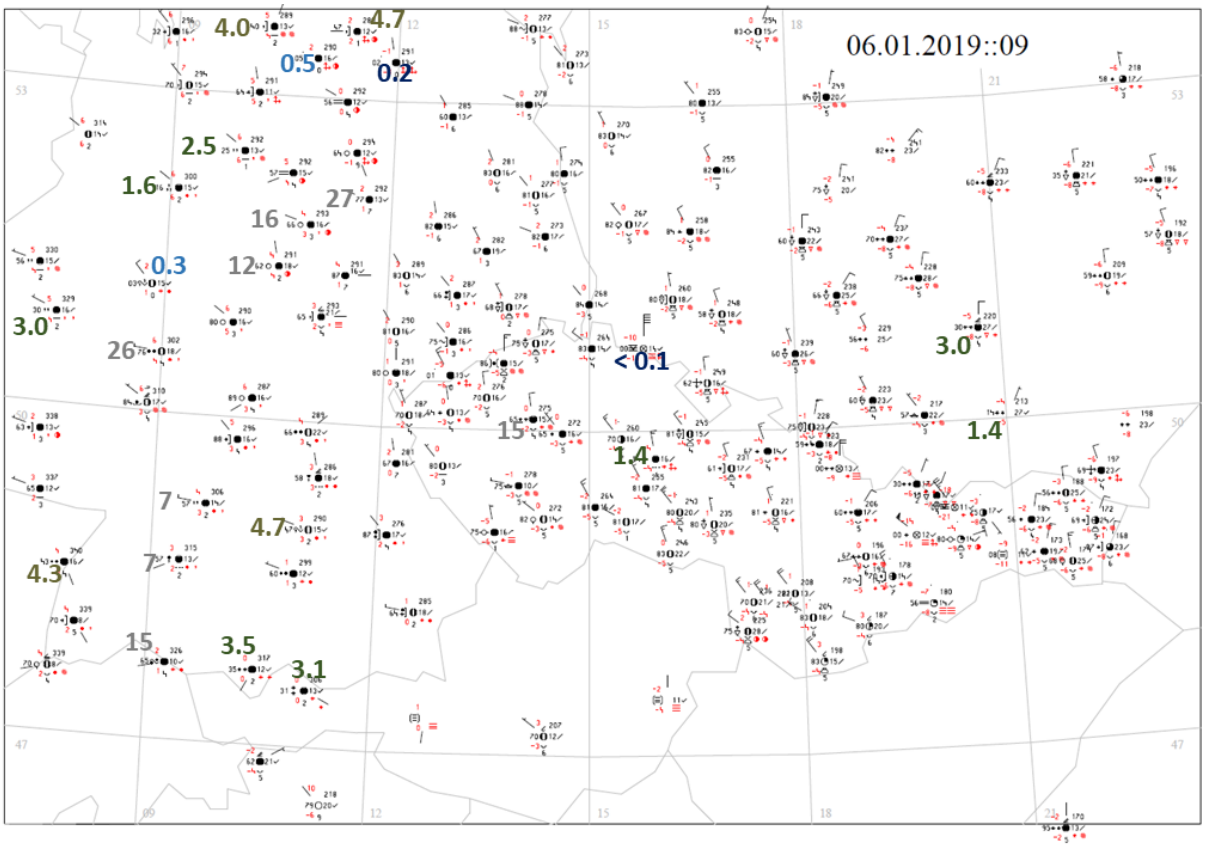

Fig. 5. Synoptic observations for the area of Central Europe for 06 January 2019 09 UTC. Some visibility records (in km) were emphasized by numbers.

Comparison with synoptic observations (Fig. 5) indicates that there were areas in Germany with low visibility but not as compact as predicted by both numerical models. In the same region, we find also stations with visibility exceeding 10 or 20 km, despite of cloudy weather and precipitation. Low visibility was reported by station on the border of Czech Republic and Poland (probably Sněžka, 1601 m high). Reduced visibility was also in the Alpine region. Fog was reported from Meiringen (Switzerland, 595 m) or Krimml (Austria, 1000m) and usually at high elevations. Somewhere the reduced visibility was due to both cloudiness and precipitation. Fog could have been also in localities, where meteorological data are absent or not distributed abroad.

In case of ALARO, one notable feature was that cloud liquid water-related visibility was always below 10 km, even if no cloudiness was predicted. Though, the threshold was 20 km, as in the case of precipitation-related visibility. It was probably due to default settings, where visibility is reduced below 4 km already in case of very low cloud liquid water content (refer to Fig. 1).

For precipitation, it can be shown that already a weak (0.1-0.5 mm/h) snowfall can reduce visibility below 2 km (Fig. 6) and moderate snowfall can cause foggy conditions as seen over the Alps or Turkey. It is probable that this only partially represents the true state of the visibility and the forecast values are lower with respect to reality.

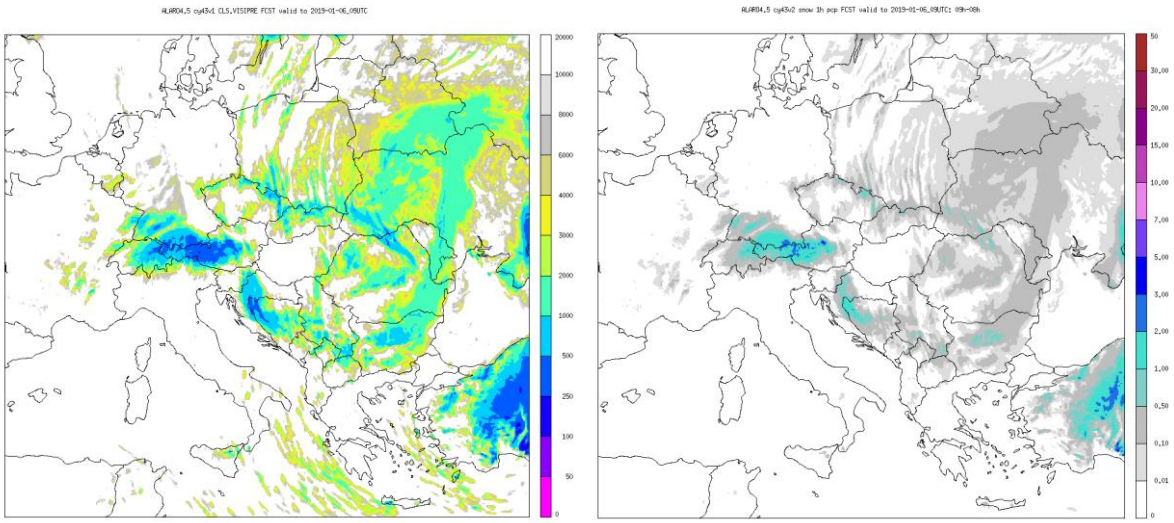

Fig. 6. a: (left) Forecast of 1h minimum visibility in precipitation (CLS.VISIPRE) from ALARO SHMU cy43t2 valid for 06 January 2019 09 UTC. 6b: (right) 1h precipitation forecast for the 08-09 UTC period.

Case 2: Fog over southern Slovakia and Hungary

As we could see, cases with appearance of both radiation fog and large-scale precipitation are difficult to evaluate. For evaluation, those situations are ideal, where fog was created largely due to radiative cooling in relatively stationary conditions (e.g. with surface anticyclone) and its distribution is relatively homogeneous, covering large areas. This could be observed on 9 November 2018 over Slovakia and eastern part of Hungary (Fig. 7).

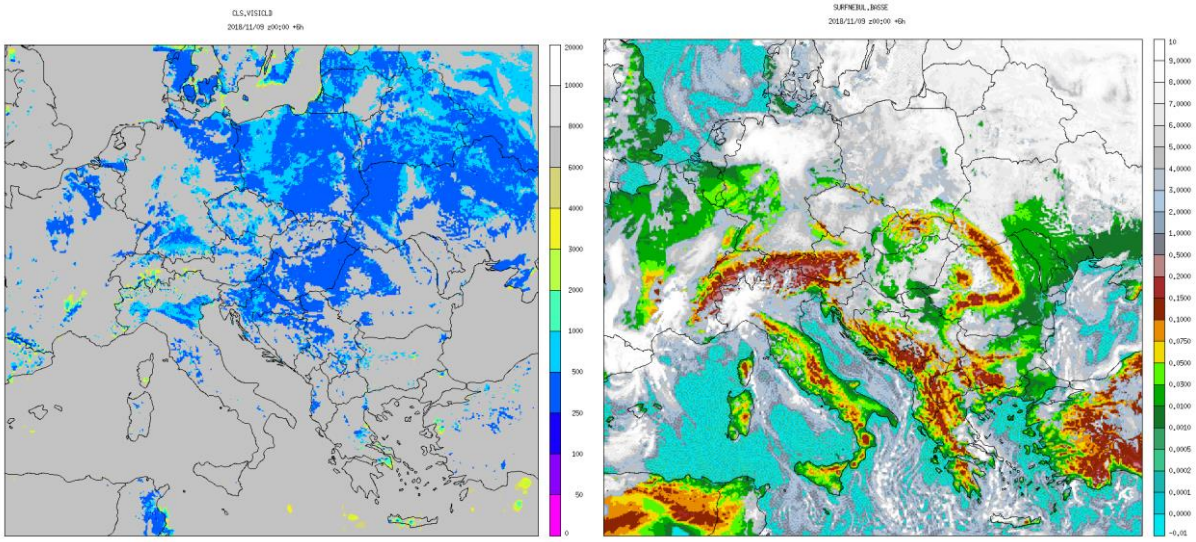

Fig. 7. a: (left) Forecast of 1h minimum visibility (m) in clouds (CLS.VISICLD) from ALARO SHMU cy43t2 for 09 November 2018 06 UTC and for default setting. b: (right) Forecast of low cloudiness coverage (grey shades, unit is 1/10, color shades for values below 1 show the background orography) valid for the same date and time.

The forecast of visibility is generally in agreement with the low cloudiness coverage, though, fog can be detected also if the cloud coverage is below 10 tenths of sky covered (we tested minimum visibility in the previous 1h, while cloudiness is instantaneous). It is noteworthy that visibility below

250 m is very rare, usually represented only by seldom points. Besides Slovakia and Hungary, fog was predicted for Po-valley and large parts of Poland or Ukraine and also for Tunisia.

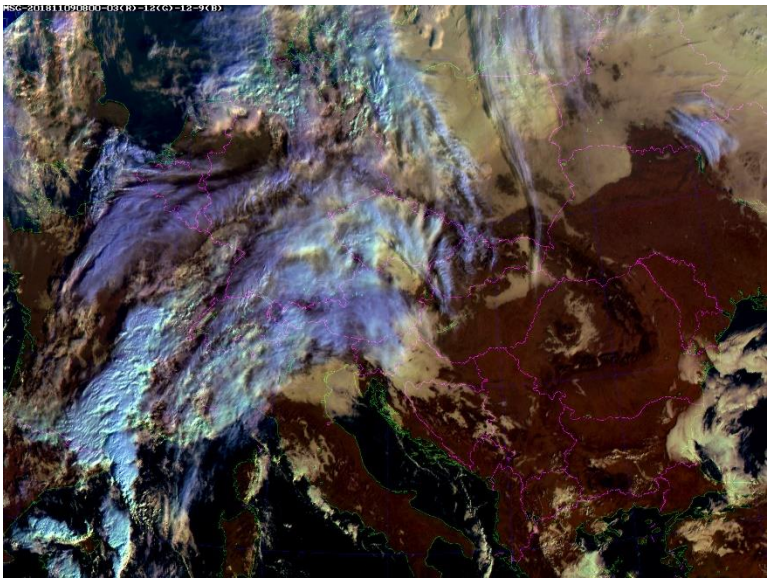

Fig.8. Meteosat 8 (MSG) Natular color RGB image valid for 09 November 2018 08 UTC (there were no big changes in distribution of low clouds between 06 and 08 UTC).

Comparison with satellite imagery (Fig. 8) shows that fog (or low clouds) were present over Slovakia and Hungary, in Carpathian mountains in Romania, Po-valley and over big parts of Poland or Belarus. It can be seen that the model overestimated the area covered by fog over Hungary (only the northeastern part of the country had fog).

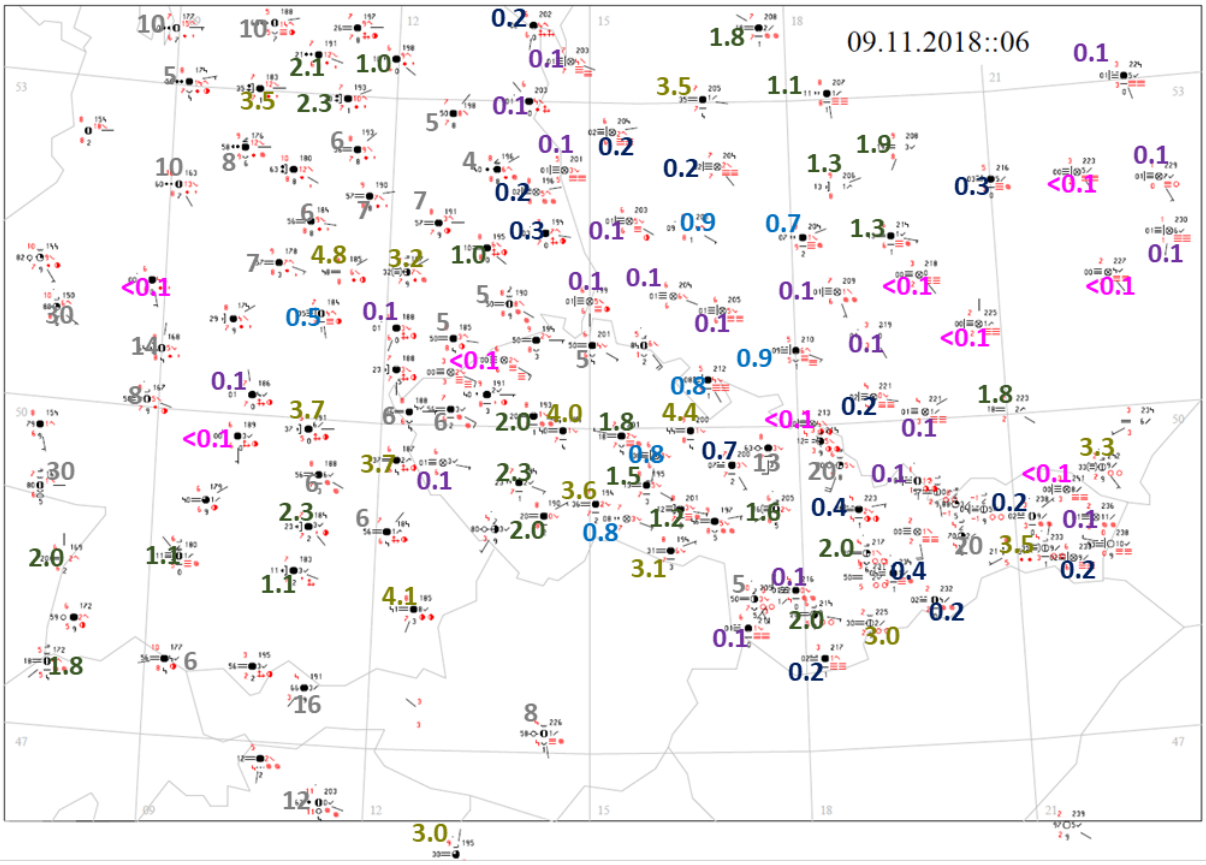

Fig. 9: Synoptic observations for the area of Central Europe for 09 November 2018 06 UTC. Visibility (numbers) is in km.

The synoptic observations (Fig. 9) indicate that fog occurred in large area of Poland and visibility was reduced to 100m or even less at many places. Fog occurred also in Germany (mainly in its eastern part) and locally also in the Czech Republic. Even if no fog, the visibility was reduced at many places, exhibiting values between 1 and 4 km. The ALARO model for some reason did not match these "interfaces", there are rather sharp gradients in visibility, which can be found in the cloud liquid water content (MAXCLWC), too. As mentioned earlier, the default setting of the model was not capable to predict very low visibility, which was actually observed at many stations (not only in mountains but mainly at lowland areas of Poland). This is a systematic overestimation related to setting of cloud liquid water and visibility relationship (1) and (2). Thus, we did tests with coefficients COEFFEXTQ and COEFFPWRQ as for Sekula-CASE1 and with settings proposed in papers of Gultepe. We also produced the CLS.VISICLD2 parameter showing almost instantaneous visibility (minimum for the last 6 min.). This was switched on with LXVISI=.T. in NAMXFU and with NVISIPERIOD2=360.

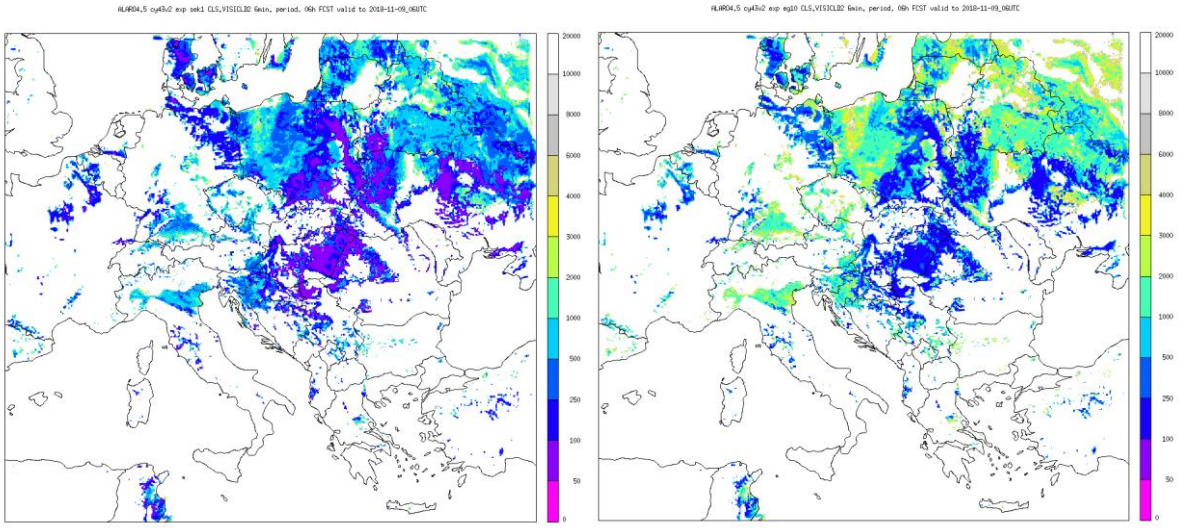

Fig. 10. a (left): Forecast of 6 min. minimum visibility (m) in clouds (CLS.VISICLD2) from ALARO SHMU cy43t2 for 09 November 2018 06 UTC and for settings of Sekula-CASE1. b (right): the same, except for the setting emulating the relationship described in Gultepe (2010).

On the Fig. 10a one can see that the predicted visibility values decreased with respect to the default setting (refer to Fig. 7). There occurred places with visibility below 100m as it was also observed at certain stations. The background low (< 4km) visibility disappeared. Qualitatively similar was the test with emulated Gultepe (2010) function (Fig. 10b). The visibility in areas of fog was not as low (usually always above 100m) and smaller area was covered by fog. Other settings (Gultepe 2006, 2007) produced similar result. The Sekula-CASE1 showed generally better fit with observations (so far only upon subjective comparison).

Case3: Visilbility reduced in strong convective rain (Czech Republic, Slovakia)

On 28 May 2019 long lasting, heavy convective rain occurred over western Slovakia and over the eastern part of the Czech Republic.

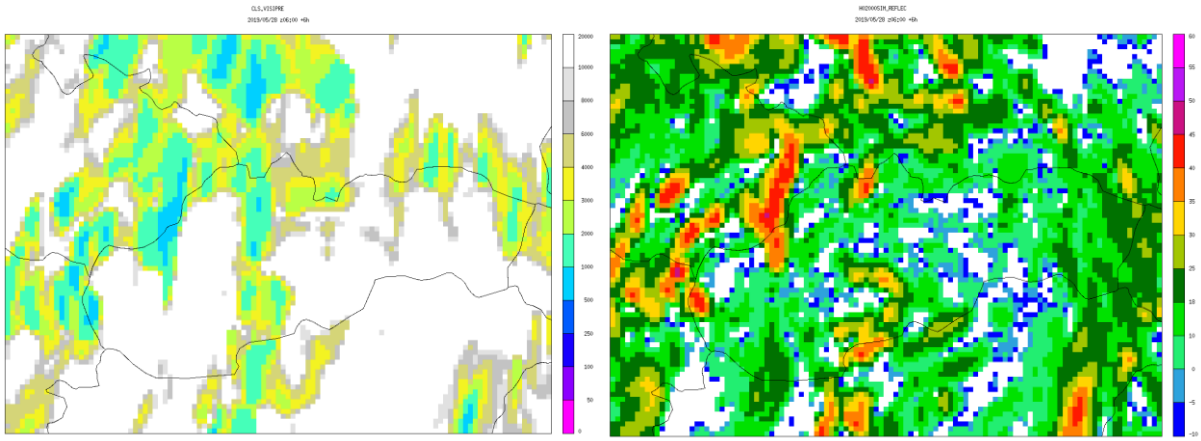

Fig. 11. a (left): 6h forecast of 1h minimum visibility (m) in precipitation (CLS.VISIPRE) from ALARO SHMU cy43t2 valid for 28 May 2019 12 UTC. b (right): Forecast of the simulated radar reflectivity (dBz) for 2 km height over the terrain valid for the same time.

On the Fig. 11 one can see that visibility was reduced in forecast heavy convective rain. Usually, visibility dropped below 1 km in case of simulated reflectivity exceeding 40 dBz.

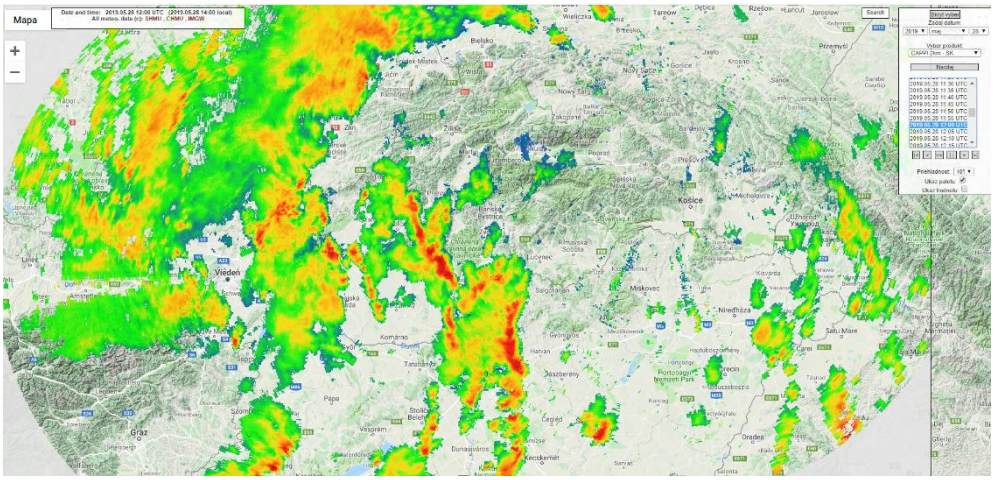

Fig. 12: Field of 2km CAPPI radar reflectivity over Slovakia and its neighbourhood on 28 May 2019 12 UTC.

On the Fig. 12 one can see that such intense convective cells really developed, although their distribution was different. The forecasts of 1h precipitation (up to 10-15mm) were also close to analysed values (not shown). Unfortunately, there was no observation at synoptic station at that time confirming that the visibility would drop below 1 km during heavy rain. It can be expected that this rather happens in relatively small (currently subgrid) areas of the heaviest precipitation. Another possibility is development of cloudiness/fog from evaporating precipitation – which is usually not predicted and it is rather a subgrid phenomenon as well.

Experiencies with test implementation in the 2 km resolution ALARO model

A pre-operational implementation of the visibility products was prepared for the 2 km horizontal resolution ALARO model (Martin Dian, Oldřich Španiel, SHMÚ). Forecasts of visibility became regularly available since late August 2019. The 2 km model uses the same cycle (Cy 43 t2 bf10) as it was in case of the 4.5 km resolution tests presented above.

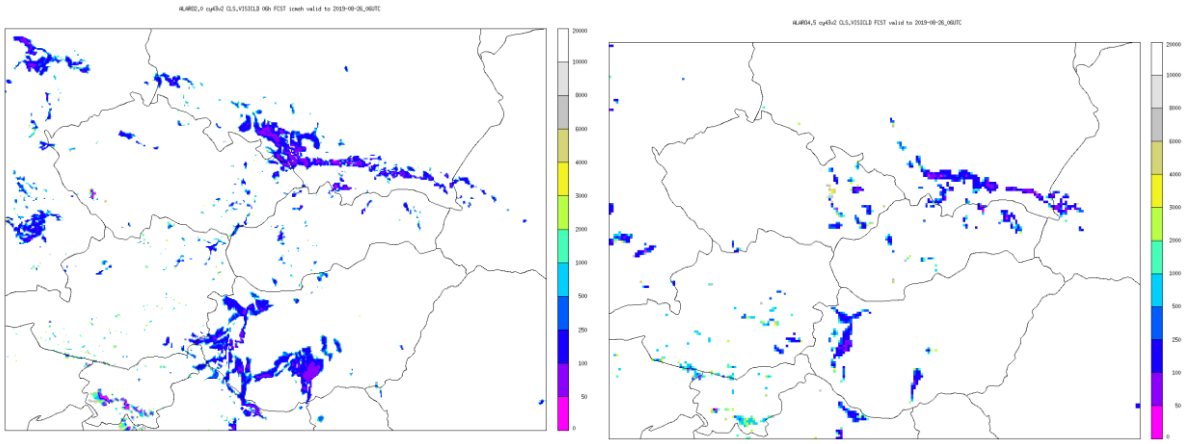

Fig. 13: 6h forecasts of visibility in clouds (CLS.VISICLD) valid for 26 August 2019 06 UTC in ALARO with 2 km resolution (left) and 4.5 km resolution (right).

Despite the fact that August is not typically a month with very frequent appearance of fog in Slovakia and its surroundings, the model forecast fog at many places, even for relatively large, compact area in Hungary or southern Poland (Fig. 13). Though, most of the fog was dissolved during the daytime.

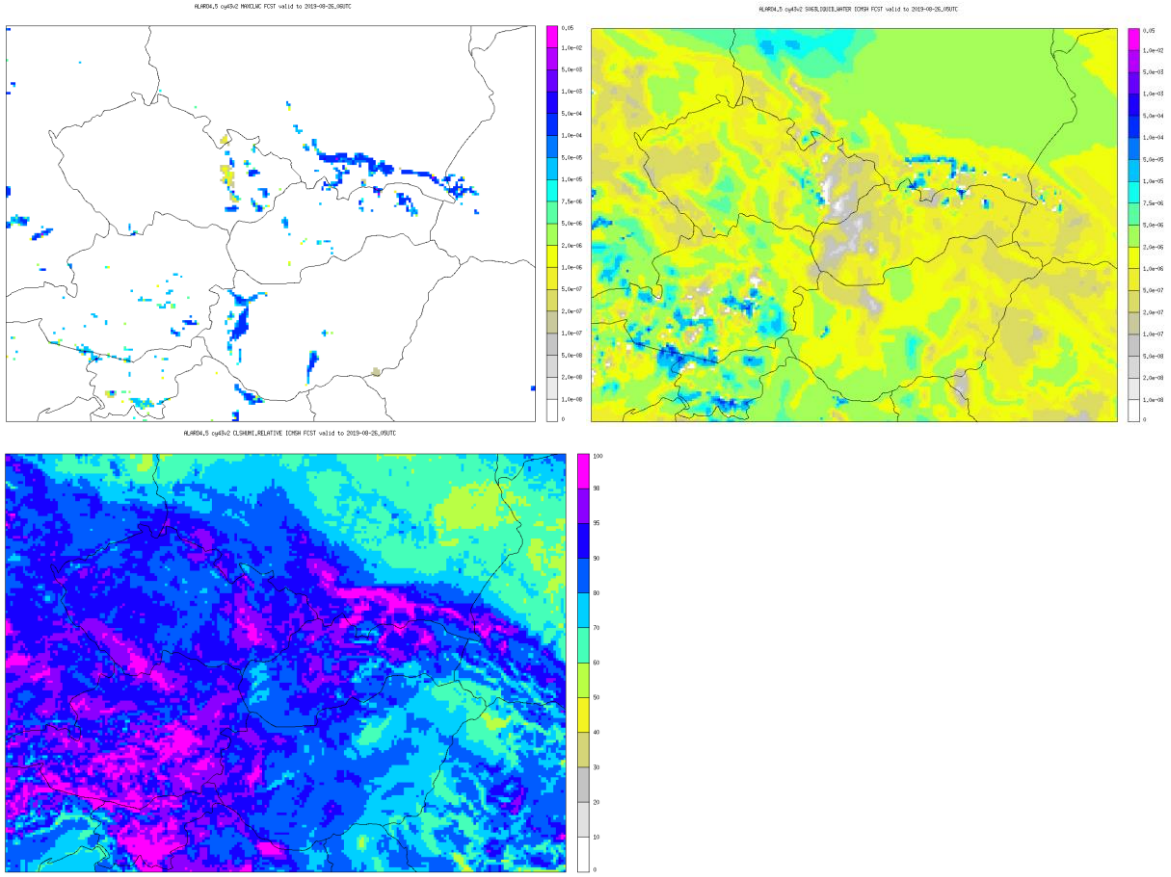

Fig. 14: Upper left: 6h forecast of MAXCLWC (1h max. PQLI) valid for 26 August 2019 06 UTC in ALARO 4.5 km resolution. Upper right: 5h forecast of cloud liquid water (PQL) at 63 (last) model level valid for 26 August 2019 05 UTC. Bottom: 5h forecast of 2m relative humidity valid for 26 August 2019 05 UTC.

Some meteorological stations reported fog in the morning but it was mostly shallow (with recognizable sky, etc.). In the 4.5 km model, the territory affected by fog was not as big as in the 2 km run. The large extension of fog in the presented forecasts could be also explained by high near-

surface humidity caused by previous intense convective precipitation. Nevertheless, there is also a confusion, which cloud liquid water content (PQL or PQLI) described better the real conditions. The fields of PQL and PQLI are sometimes even contradictive, which can be possibly also a result of interpolations of PQL. Note for example the area of western Slovakia and Hungary on Fig. 14, where the values of PQL were rather low compared to MAXCLWC parameter inferred from PQLI. However, it seems that PQLI better fits the distribution of certain humidity fields, e.g. that of the 2m relative humidity, which was close to saturation at many places.

Comparison with METAR data

The findings described above inspired us to compare the cloud liquid water content and visibility forecasts with METAR records from several central European countries (Fig. 15). We selected 16 days with fog (Table 2) occurring in various parts of the region and at different time of the year (mostly in autumn and winter).

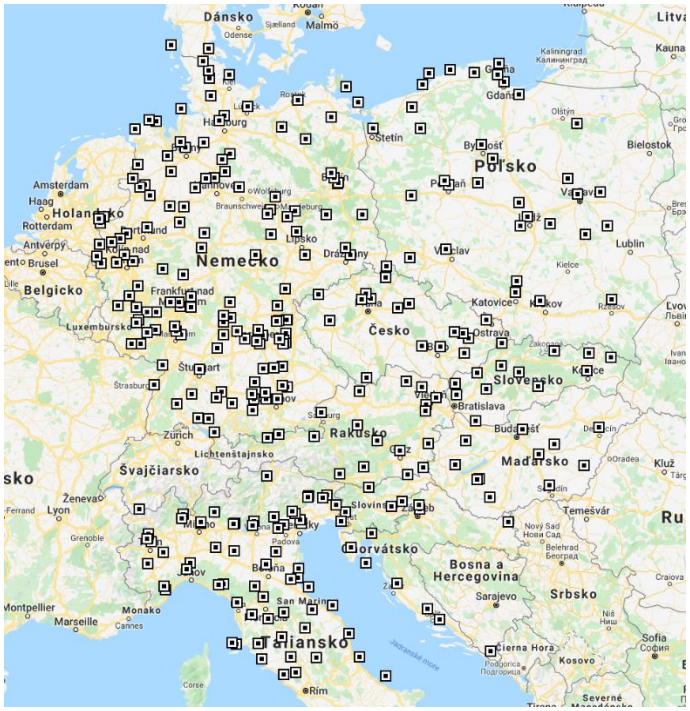

Fig. 15: METAR stations used for the evaluation of the visibility parameterisation

Date of the run:	Location (countries, where problems with fog were reported)	occurrence	run	Run as dynamic adaptation	Run with CANARI analysis
01/01/2017 fog	D, CZ, SK	06 UTC	00 UTC	Y	N
13/02/2017 fog	H, SK	06	00	Y	N
14/02/2017 fog	H, SK		00	Y	N
23/02/2017 fog	I		00	Y	N
21/03/2017 fog	I	06-08	00	Y	N

10/10/2017 fog		06 UTC	00	Y	N
18/10/2017 fog	D, I, HR		00	Y	N
25/11/2017 fog	H, CZ		00	Y	N
02/01/2018 fog	SI	01	00	Y	N
11/01/2018 fog	SK, CZ, I		00	Y	N
04/11/2018 fog	H, SK, CZ, D		00	N	Y
05/11/2018 fog	H, SK, CZ, D		00	N	Y
09/11/2018			00	N	Y
29/12/2018 fog	I		00	N	Y
06/01/2019	D	06	00	N	Y
26/08/2019	SK, H		00	N	Y

Table 2: List of situations with fog, investigated during the evaluation

The concept of possible adjusting of the cloud liquid water – visibility relationship was based on the linearization of the formulas (1) and (2). In such form one could write:

$$\ln\left(\frac{z_s\, z_c}{V} - \beta_0\right) = \ln C_{EQ1} + C_{PQ1} \ln(z_s\, \rho\, q_{lwc}) \quad (5)$$

$$M_c = \rho q_{lwc}\,, (6)$$

where V is visibility in m, M_c is the cloud liquid water in kgm^{-3} represented by parameter MAXCLWC and C_{EQ1} , C_{PQ1} are the COEFFEXTQ(1), COEFFPWRQ (1) coefficients, which we tried to adjust. Visibility is from METAR observations, while M_c data are from model forecasts, since this parameter is commonly not measured at meteorological stations.

At the beginning, we had to solve the problem of representativeness of both METAR observations of visibility and M_c data. The visibility in the METAR report is considered to be a prevailing visibility, which in aviation means a „measurement of the greatest distance visible throughout at least half of the horizon, not necessarily continuously“. When horizontal visibility is not the same in different directions, and when visibility is fluctuating rapidly and the prevailing visibility cannot be determined, the lowest visibility should be reported (WMO-No.782, 2019). It must be also underlined that METAR reports consist only visibility observations below 10000 m, higher visibility is not coded (unlike in SYNOP reports). The definition above already reveals that using spatially very distant METAR reports can be problematic for evaluation, since the variability of the visibility can be high. Though, we selected situations with rather similar conditions over large areas with frequent occurrence of fog or decreased visibility. During the evaluation, we considered the METAR observation to represent average visibility conditions for bigger area around the airport. Further problem was, which M_c data to take as relevant for comparison. Using single forecast from nearest neighbour grid-point to the airport could be problematic. We expected high forecast uncertainty in predicting fog. From forecaster's point of view, even if the fog area is shifted with respect to its real position, it still carries valuable information about the possibility of the event. Thus, we considered a broader area around the METAR station, consisting of maximum 81 grid-points (Fig. 16). If fog was observed, we attributed the mean visibility (or M_c) of the forecast fog within the area to the visibility at the METAR station. In case that no fog was observed (visibility exceeding 1000 m), we calculated the average visibility (M_c) in areas outside fog. The thresholds for cloud were 5 10^{-6} (lower threshold) and 1 10^{-5} kgm^{-3} (upper threshold). It turned to be important that at least 9 grid-points were taken

for calculations to avoid comparisons with small artefacts, not necessarily representative for wider area. We also filtered out those grid-points, which model height differed from the height of the observation by more than 200 m. The time-span between the forecast and observation was ±1 hour. We compared 2-12 h forecasts from 00 UTC runs with minimum METAR visibility in the relevant 2 h period around the forecast time (since M_c is also not an instantaneous value but 1h maximum of cloud liquid water). Analyses and 1h forecasts were not used due to spin-up of hydrometeor calculation in case of dynamic adaptation.

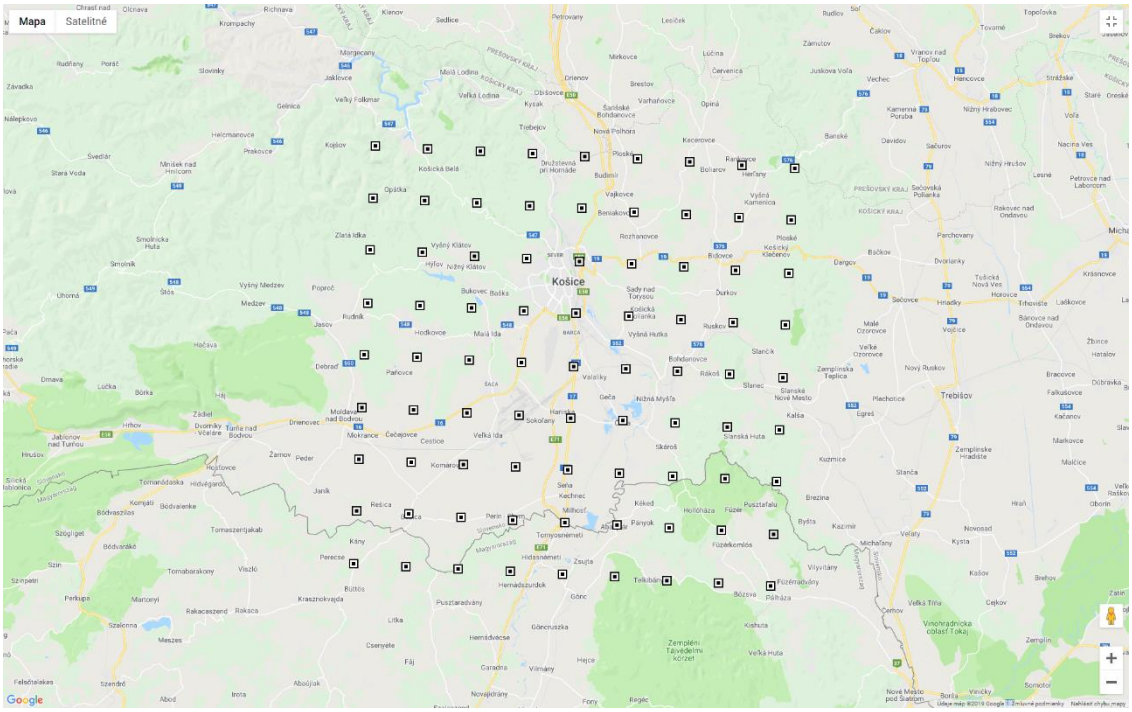

Fig. 16: Area around the METAR observation point at the Košice airport marked by model grid-points considered in forecast visibility and M_c calculations.

We also included an analogical parameter to M_c in model calculations to represent the cloud liquid water content from microphysics (ZQL in aplpar.F90). We called this new parameter as MAXCLWQ (M_q) and it represents the maximum of cloud liquid water in kg m-3 units within the previous hour:

$$M_q = \rho q_{lwc} \quad (7)$$

We applied the same linearized equation (5) to investigate the relationship between the cloud liquid water and visibility.
For both M_c and M_q we calculated the logarithmic terms in the eq. 5. We collected 3100 valid records with both observation and forecast for M_c and 9463 records for M_q. The results depicted in Fig. 17 indicate that there is a very high spread in the forecast M_c for a given visibility class (most of the visibility observations are not given in a continuous form but assigned to a pre-defined interval). However, one can clearly distinguish between the areas with no cloud (mist) and events with fog. The results were similar for M_q, except there were more records for non-cloudy areas. From the graphs one could hardly conclude that the relationship between the two logarithmic terms is linear. The correlation coefficient for the proposed linear tendency is about 54%, which is rather low. This is both due to high forecast uncertainty of the predicted cloud liquid water and probably also due to high spatial variability of this parameter in general. Nevertheless, the linear regression gave us a guess about their relationship, which is comparable with setups described in the technical part.

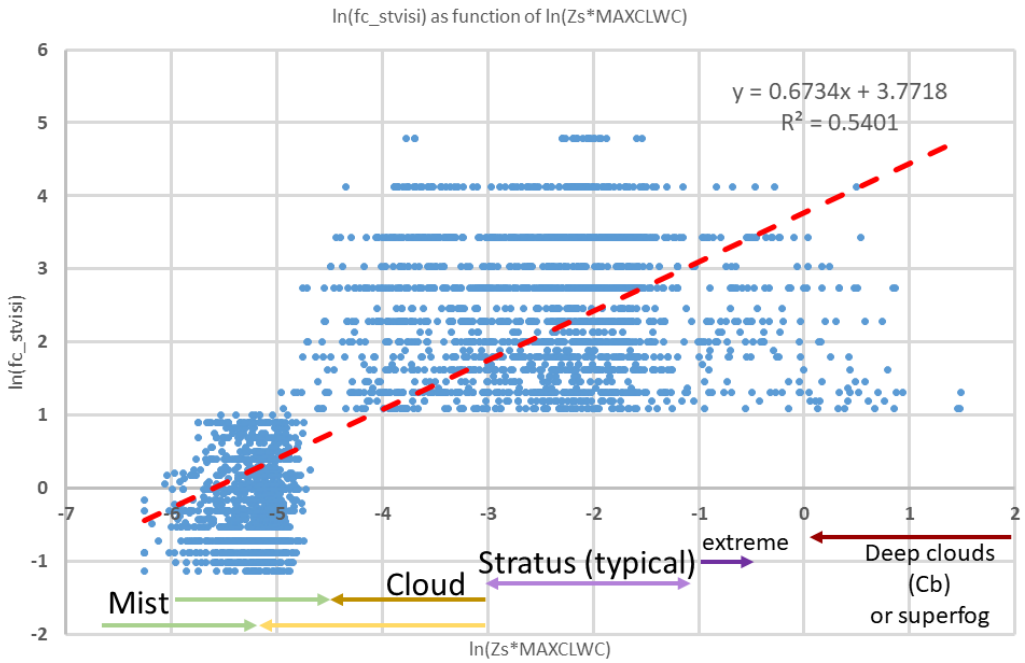

Fig. 17: Relationship between the logarithmic terms at the left and right hand side of Eq. 5 for M_c (MAXCLWC) for all relevant records (non-cloudy areas or fog present in both model forecasts and at the evaluated station) depicted by dots. The x-axis shows the term related to cloud liquid water. Respective categories (Mist, Stratus, etc.) were shown upon values published in the literature. The threshold for cloud is not a certain value, thin clouds can form already by relatively low liquid water content, thus both lower and upper thresholds (5 10^{-6} – 1 10^{-5} kg m^{-3}) used in this study were emphasized.

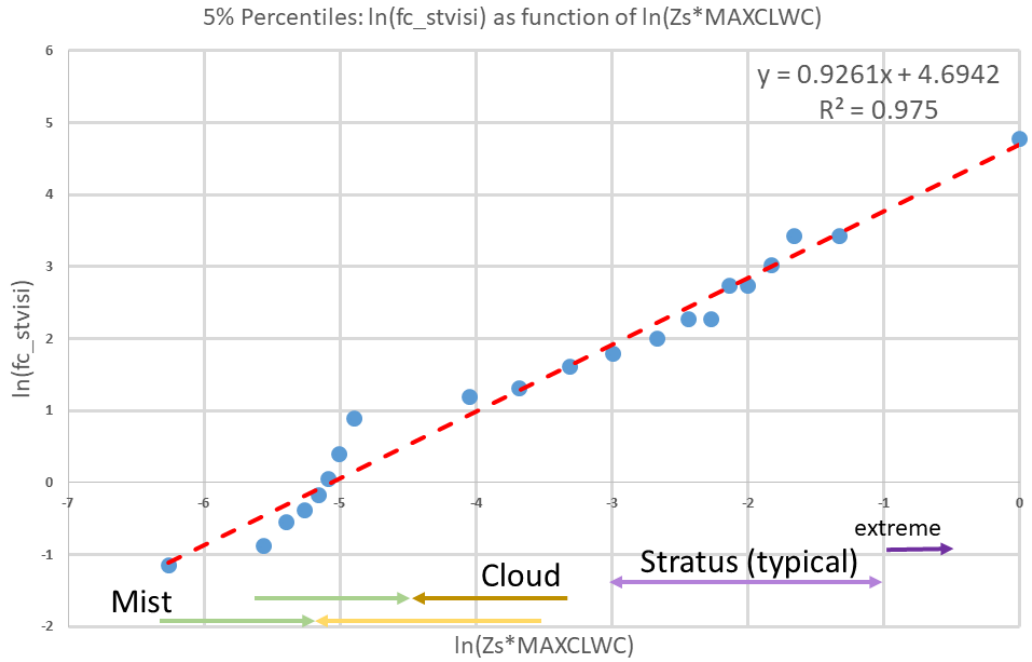

Fig. 18: As in Fig. 17 but only for the percentiles (by 5%) of the distribution of the visibility and M_c functions. The extreme M_c values exceeding 1 10^{-3} kg m^{-3} were omitted.

Another idea was to concentrate on the overall statistical distributions of visibility and cloud liquid water rather than on respective values and areas. If we expect that there is a close relationship between these quantities (and little dependency on other parameters), their statistical distribution should be similar. Thus, the quartiles, medians, etc. of one parameter (e.g. visibility) should have

their counterparts in the statistical distribution of cloud liquid water and derived variables. We calculated the percentiles of the distribution of the logarithmic terms related to visibility and M_c (M_q) by 5% (Fig. 18). The output of this statistics resembles much more a linear relationship with correlation coefficient up to 97.5%. Though, in case of mist we could see that the visibility drops steeper with increasing cloud liquid water as predicted by the final relationship. Very similar results were obtained also by evaluating the 2% or 10% percentiles. Similar distributions and relationships were found also for M_q (not shown).
Although we found that the distributions of the predicted cloud liquid water and visibility are similar, the frequency distributions show also some substantial differences.

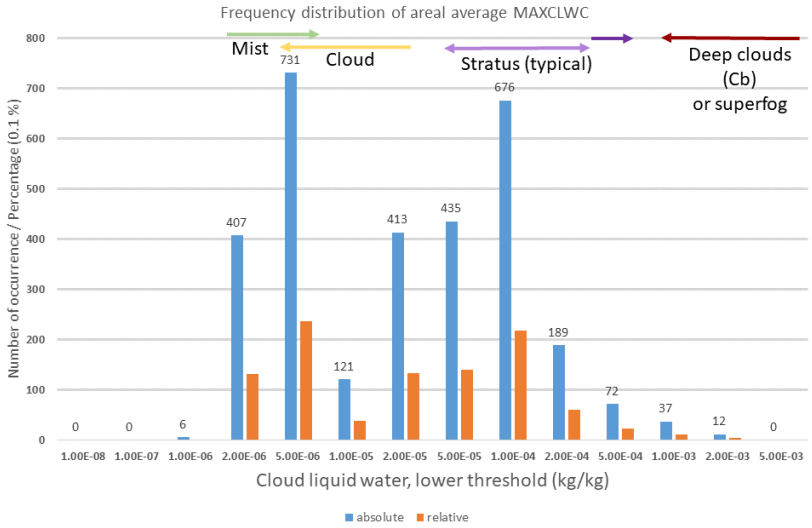

Fig. 19: Frequency distribution of M_c (kg m^{-3}) showing absolute occurrence number and relative occurrence with respect to all events (%). The x-axis shows the lower threshold of M_c class, e.g. the column assigned to 2 10^{-6} kg m^{-3} means number of occurrence between 2 10^{-6} and 5 10^{-6} kg m^{-3}.

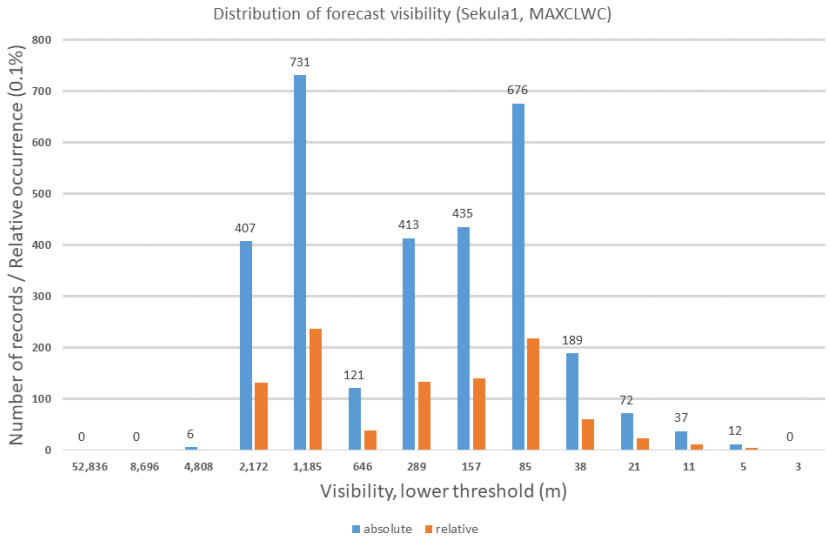

Fig. 20: Frequency distribution of forecast visibility (m) calculated from M_c upon the setup of Sekula1 (from Stoelinga, 1999).

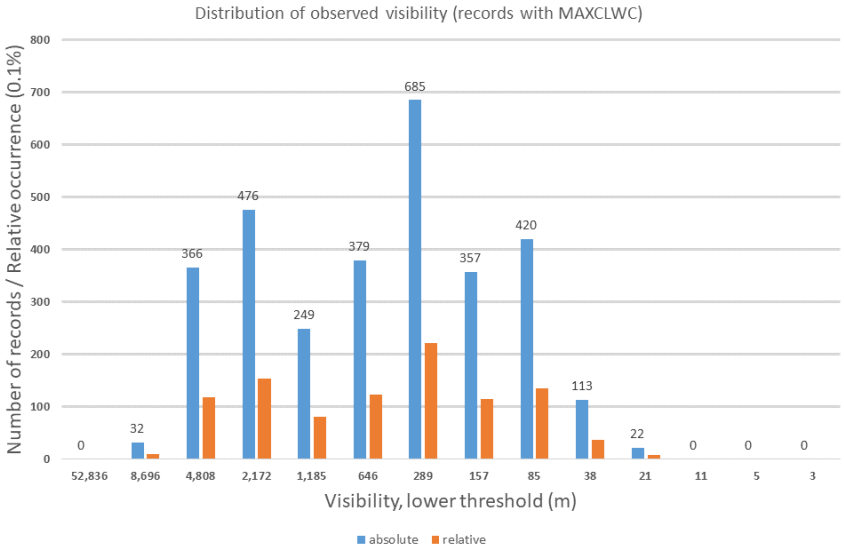

Fig. 21: As in Fig. 20 but for the observed visibility in METAR reports.

It can be seen that for M_c (MAXCLWC) also very high values (exceeding 1 10^{-3} kg m^{-3}) were forecast (Fig. 19). Such values were observed in deep precipitating clouds (e.g. in thunderstorms) or in case of the so-called superfog (Achtemeier, 2008). However, superfog needs a strong production of aerosols (e.g. from fires) and high humidity, which was not the case for the model runs (no aerosol parameterisation) and selected situations. Although the occurrence is relatively low, it is still a significant feature because we evaluated areal average values, not single artefacts. We calculated also a corresponding visibility frequency distribution (Fig. 20) to compare with observations (Fig. 21). One could see that the forecast visibility is significantly shifted toward lower values. In the observations, the mist category cases are much more frequent and there dense fog events are not so numerous (the lower threshold for observed visibility yields 25 m).

Similarly, we evaluated the distribution of M_q (MAXCLWQ). In comparison with M_c we see higher frequency of mist cases (Fig. 22). It is uncertain, how much real are the forecasts of such small liquid water content and corresponding visibility. In the real atmosphere, mist is often preceded by presence of aerosols and solid particles (haze).

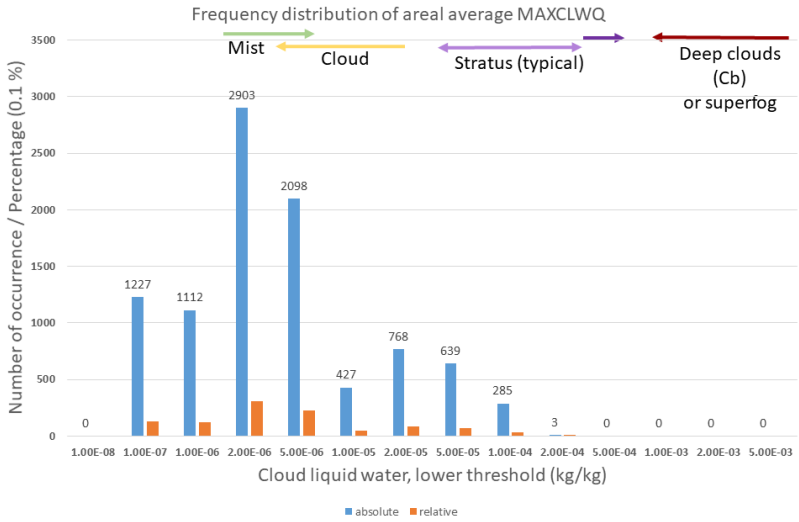

Fig. 22: As in Fig. 19 but for the parameter M_q (MAXCLWQ).

These can serve as condensation nuclei, around which microscopic water droplets develop, further reducing visibility (mist) in case the relative humidity is sufficiently high. However, this process is not included in current model parameterization. This can be also the reason for differences between the number of forecast (Fig. 23) and observed (Fig. 24) mist events. The number of events with visibility reduced to 4-10km is about three times higher compared to model forecasts. We can also see that in contrary to M_c the average values of M_q do not exceed 5 10^{-4} kg m^{-3}, which is more realistic concerning usual liquid water content in fog.

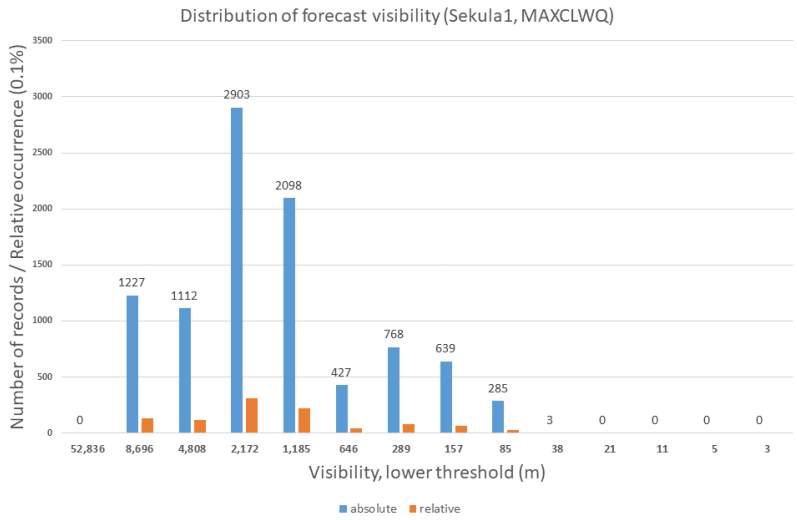

Fig. 23: As in Fig. 20 but for the parameter M_q (MAXCLWQ).

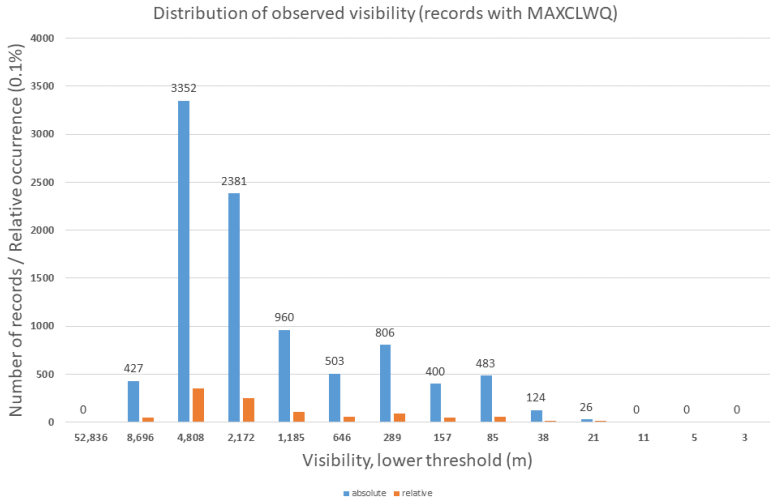

Fig. 24: As in Fig. 21 but for the evaluation of M_q. Note that the observed visibility distributions were different, because with M_q we had much bigger number of records, where both forecasts and observations could be evaluated (mainly in the "mist" category).

Finally, we plot the logarithmic visibility functions with C_{EQ1}, C_{PQ1} obtained from statistical evaluation of eq. 5 (Table 3, Fig. 25, Fig. 26). There is relatively little difference between the setups for MAXCLWC and MAXCLWQ, if we consider all lwc and visibility records as depicted in Fig. 17. This setup (denoted p3x) lies somewhere between the current code default and the "sekula1" setting. Thus, it is practically unable to forecast very low visibility (below 100m), especially not in case, we use M_q forecasts as input. As we reduce the spread and number of data to calculate the relationship, we get closer to the "sekula1" parameterization. In case of the p5x setup and MAXCLWQ we would obtain even lower visibility for the same lwc inputs (Fig. 26).

Formula abbreviation - meaning	MAXCLWC (M_c)		MAXCLWQ (M_q)	
	COEFFEXTQ(1) C_{EQ1}	COEFFPWRQ (1) C_{PQ1}	COEFFEXTQ(1) C_{EQ1}	COEFFPWRQ (1) C_{PQ1}
P3x – from all lwc and visibility records	43.4582	0.6734	43.5583	0.6558
P4x – from average lwc belonging to respective visibility classes	41.3057	0.7208	129.3601	0.871
P5x – from distribution of lwc and visibility by 5% percentile	109.3113	0.9261	185.1192	0.8569

Table 3: Coefficients of the visibility-cloud liquid water content relationship calculated from statistical evaluation and comparison of forecast *lwc* and observed METAR data.

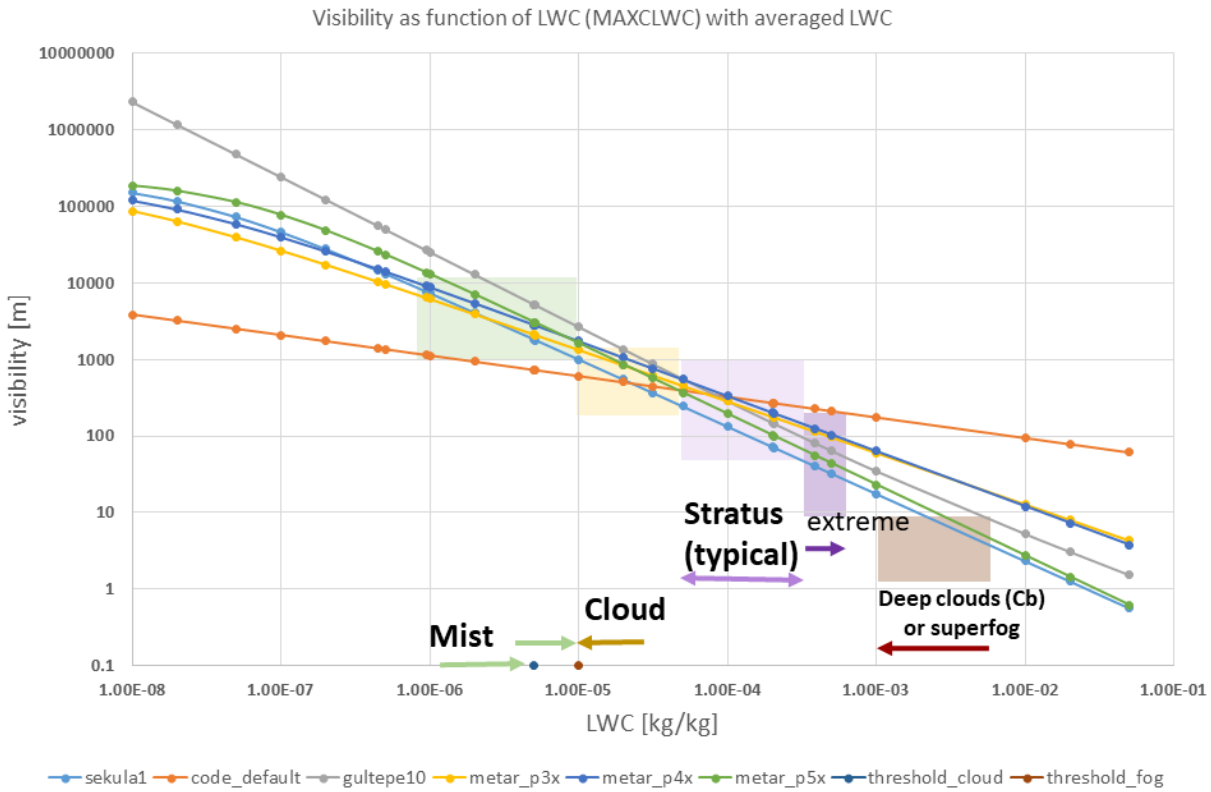

Fig. 25: Visibility (m) as function of cloud liquid water (kg/kg) only ($\beta_{ice} = 0$) as described in the report of Sekula (2018) – sekula 1 (his CASE1), default code setting (see Table 1) and emulated Gultepe (2010) relationships based on the Eq. (4). The p3x, p4x, p5x are new settings defined upon comparison with METAR observations (refer to Table3). Compare also with Fig. 2. The scales are logarithmic. The shaded areas show typical values of lwc and visibility for mist, stratus clouds or superfog as found in the literature. The setting is valid for the MAXCLWC (M_c) parameter on input.

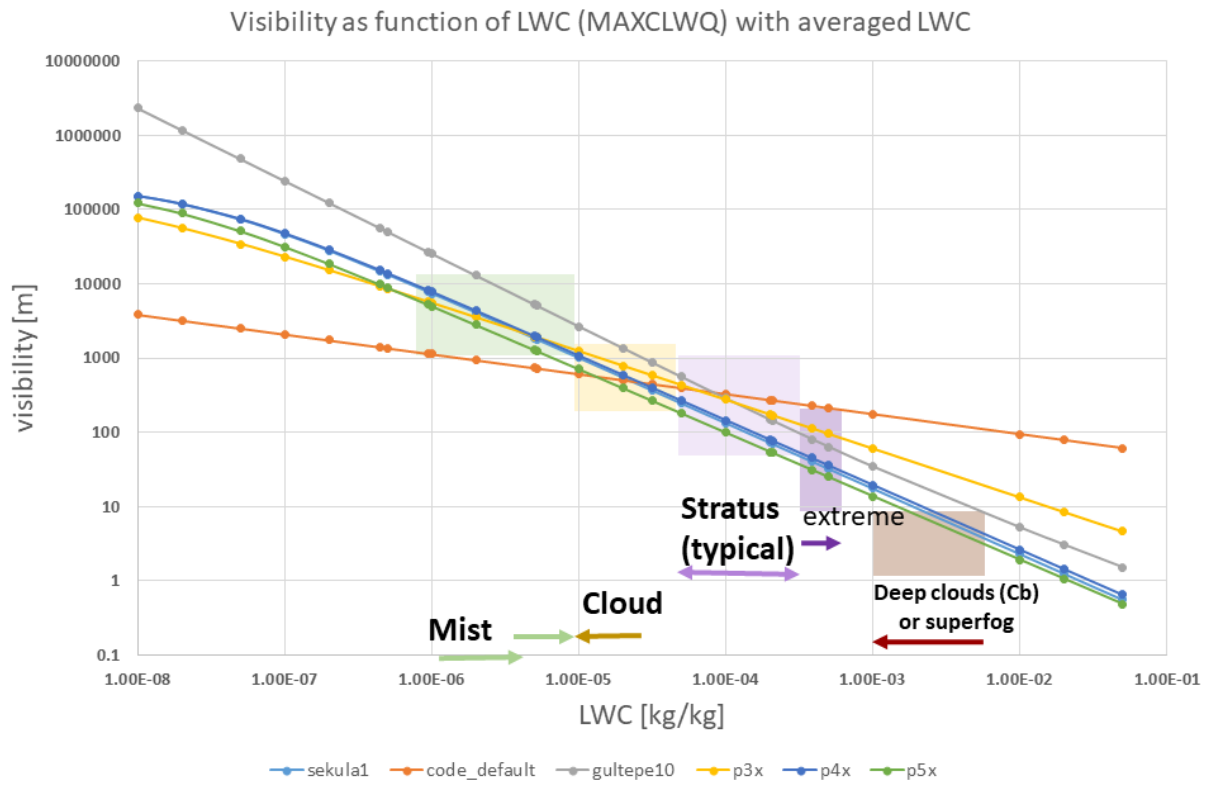

Fig. 26: As in Fig. 25 but for MAXCLWQ (M_q).

Finally, we evaluated the newly obtained functions (p3x, p5x) with respect to observations and calculated the potential scores (BIAS, MAE, RMSE, etc.) of forecasts with these settings (Table 4 and Table 5). We calculated visibility for every point around the METAR observation (as depicted in Fig. 16) but we used only areal averages for comparison (applying the minimum 9 point rule). We also calculated 2x2 contingency tables and probabilities of forecasting events like clear sky, reduced visibility (both mist and fog events), fog or dense fog. We defined dense fog as event with visibility below 100 m.

From Table 4 we can see that the probability of forecasting fog is usually below 70% and the false alarm ratio is relatively high (about 70% as well). The mean error in visibility exceeds 200 m, which is also quite high. Interestingly, the current default setting shows the best score in the fog category, perhaps, because its visibility forecast does not vary so strongly with increasing lwc compared to other schemes. On the other hand, with the default setting it was not at all possible to predict dense fog events. Similarly, in the mist category the best scores were obtained for the parameterization based on the article of Gultepe (2010), where the visibility reached higher values for the same lwc, compared with other tested parameterisations. This suggests that better scores were reached if the scheme was closer to intermediate values of visibility in the respective class. This is likely due to high forecast spread of lwc and spatial variability of the observed visibility. Thus, the verification probably does not tell us too much, whether the physical properties of the schemes are realistic, or not, above all in case of extremes. We get only very coarse information about the ability of forecasting visibility for the respective types of events. It is despite the fact that we intentionally selected cases with reduced visibility over relatively large areas and avoided regions with rugged orography.

In case of MAXCLWQ used as input the scores seem to be better than for MAXCLWC, which can be also for the above mentioned reasons. Apparently, with MAXCLWQ there is much bigger chance to forecast mist events (with almost 80% probability). On the other hand, the forecast of dense fog was possible only for the settings sekula1 and p5x with relatively poor detection capability (below 30%).

Table 4: Scores and contingency table outputs for different visibility formulas and types of events for MAXCLWC as input. The scores could not be computed for clear sky area, because visibility exceeding 10000 m is not reported in METAR. Some scores with notable performance are highlighted in each class.

class	bias	mae	rmse	Hits	False Alar	Misses	Correct ne	pod	far	csi	fbias	pc
clear sky												
sekula1	NR	NR	NR	12957	11875	535	1388	0.9603	0.4782	0.5108	1.8405	0.5362
default	NR	NR	NR	12957	11875	535	1388	0.9603	0.4782	0.5108	1.8405	0.5362
gultepe10	NR	NR	NR	12960	11925	532	1338	0.9606	0.4792	0.5099	1.8444	0.5344
p3x	NR	NR	NR	12957	11875	535	1388	0.9603	0.4782	0.5108	1.8405	0.5362
p5x	NR	NR	NR	12957	11875	535	1388	0.9603	0.4782	0.5108	1.8405	0.5362
mist+fog+dense fog												
sekula1	-1818.89	2164.0	2838.7	5246	1303	8017	12189	0.3955	0.1990	0.3602	0.4938	0.6517
default	-3308.37	3308.4	3876.6	5570	1501	7693	11991	0.42	0.2123	0.3773	0.5331	0.6564
gultepe10	-689.934	2034.1	2601.6	5225	1322	8038	12170	0.394	0.2019	0.3582	0.4936	0.6502
p3x	-1998.7	2266.6	2957.8	5356	1401	7907	12091	0.4038	0.2073	0.3652	0.5095	0.6521
p5x	-1016.48	2063.8	2639.1	5355	1387	7908	12105	0.4038	0.2057	0.3655	0.5083	0.6526
fog+dense fog												
sekula1	-103.262	238.1	307.8	1821	4028	1179	19727	0.607	0.6887	0.2591	1.9497	0.8054
default	-16.2599	221.4	271.4	2011	5022	989	18733	0.6703	0.7141	0.2507	2.3443	0.7753
gultepe10	-44.0166	224.9	288.2	1540	3191	1460	20564	0.5133	0.6745	0.2487	1.5770	0.8262
p3x	10.8233	240.1	302.0	1801	3928	1199	19827	0.6003	0.6856	0.2600	1.9097	0.8084
p5x	-65.3512	243.6	312.0	1766	3728	1234	20027	0.5887	0.6786	0.2625	1.8313	0.8145
dense fog												
sekula1	-1.4363	26.4	33.5	196	1793	514	24252	0.2761	0.9015	0.0783	2.8014	0.9138
default	NR	NR	NR	NR	NR	NR	NR	NR	NR	NR	NR	NR
gultepe10	-44.7303	44.7	48.8	16	339	694	25706	0.0225	0.9549	0.0153	0.5000	0.9614
p3x	-31.0758	31.1	36.1	13	271	697	25774	0.0183	0.9542	0.0133	0.4000	0.9638
p5x	-13.5495	24.2	35.3	55	600	655	25445	0.0775	0.9160	0.0420	0.9225	0.9531

Table 5: As in Table 4 but for MAXCLWQ as input.

class	avgbias	avgmae	rmse	Hit nr	False aları	Miss nr	Correct ne	pod	far	csi	fbias	pc
clear sky												
sekula1	NR	NR	NR	7726	6632	5766	6631	0.5726	0.4619	0.3839	1.0642	0.5366
default	NR	NR	NR	5353	4916	8139	8347	0.3968	0.4787	0.2908	0.7611	0.5121
gultepe10	NR	NR	NR	10068	8402	3424	4861	0.7462	0.4549	0.4599	1.3690	0.5580
pc3x	NR	NR	NR	6562	5785	6930	7478	0.4864	0.4685	0.3404	0.9151	0.5248
pc5x	NR	NR	NR	7279	6354	6213	6909	0.5395	0.4661	0.3668	1.0105	0.5303
mist+fog+dense fog												
sekula1	-1597.7	2554.9	3164.5	10276	8733	2987	4759	0.7748	0.4594	0.4672	1.4332	0.5620
default	-3617.9	3631.8	4282.5	11303	10435	1960	3057	0.8522	0.4800	0.4770	1.6390	0.5367
gultepe10	-624.0	2172.0	2700.0	9046	6528	4217	6964	0.6820	0.4192	0.4571	1.1742	0.5984
pc3x	-1377.5	2663.5	3285.6	10861	9607	2402	3885	0.8189	0.4694	0.4749	1.5432	0.5511
pc5x	-1907.0	2616.8	3250.3	10453	9099	2810	4393	0.7881	0.4654	0.4674	1.4742	0.5549
fog+dense fog												
sekula1	-54.0	241.7	306.2	2007	7575	993	16180	0.6690	0.7905	0.1898	3.1940	0.6798
default	92.8	257.8	305.2	2477	14596	523	9159	0.8257	0.8549	0.1408	5.6910	0.4349
gultepe10	61.8	243.8	291.7	1526	3160	1474	20595	0.5087	0.6743	0.2477	1.5620	0.8268
pc3x	58.2	242.1	293.8	1865	5988	1135	17767	0.6217	0.7625	0.2075	2.6177	0.7338
pc5x	-69.3	251.4	317.9	2163	9591	837	14164	0.7210	0.8160	0.1718	3.9180	0.6102
dense fog												
sekula1	7.9	17.6	25.0	63	283	647	25762	0.0887	0.8179	0.0634	0.4873	0.9652
default	NR	NR	NR	NR	NR	NR	NR	NR	NR	NR	NR	NR
gultepe10	NR	NR	NR	NR	NR	NR	NR	NR	NR	NR	NR	NR
pc3x	NR	NR	NR	NR	NR	NR	NR	NR	NR	NR	NR	NR
pc5x	2.9	21.9	27.9	152	997	558	25048	0.2141	0.8677	0.0890	1.6183	0.9419

It is probable that one would need much higher spatial density of observations of both visibility and cloud liquid water content to provide a correct verification. Currently it seems that one of the best options is to use the setting of "sekula1", which does not generate much worse scores than other parameterisations in the respective classes and it can provide forecasts of dense fog events. Some "intermediate" settings between "sekula1" and the current default (like pc3x, emulated Gultepe 2010) could be used if one would like to avoid too many false alarms in the dense fog category and still keep possibility to predict visibility close to 100 m. It must be emphasized that currently none of the schemes is capable to predict realistically visibility reduced below 10 m. If such cases occur, it is due to too high forecasts of lwc (observed only in case of MAXCLWC on input) and not because of the visibility-lwc relationship. Thus, retuning of this part of the parameterization related to "radiation cloudiness" (parameter RPHI0) could be suggested (personal communication with Radmila Brožková and Ján Mašek).

Preliminary conclusion:

By now, the results obtained from the visibility parameterisation for both cloud and precipitation seem to be reasonable to some extent, the products evidently correspond to other forecasts of meteorological parameters (low cloudiness, radar reflectivity) indicating reduced visibility. The forecast quantities are more problematic, since the setting is inferred from few known published experiments. Such measurements can depend on the used device and on the local conditions, or on the site of the experiment (tower, ground, etc.). As we could see, there are significant differences between the proposed formulas, even if dependent on only few parameters (it is mostly only other way to express the quantity of the cloud liquid water content). Actually, visibility or the extinction coefficients could be influenced by other meteorological parameters, directly not involved (wind, turbulence) and by presence of aerosols (not available in the model yet).
We tried to set the coefficients COEFFEXTQ, COEFFPWRQ upon observed visibility (upon central European METAR observations) and very short range forecasts of cloud liquid water content measurements. However, it seems that the spatial variability of the real visibility and uncertainty in the cloud liquid water content makes such tuning difficult. It is noteworthy that the relationships between the statistical distributions of the two compared parameters are very close to the parameterization, which was proposed in scientific papers (e.g. Kunkel, 1984, Stoelinga and Warner, 1999) and based upon direct measurements. At least, the statistical evaluation indicates that it is probably the current radiation cloudiness scheme, which predicts too high cloud liquid water contents near surface and it probably should be retuned toward lower values, if possible. This is important above all in the higher-resolution models. Nevertheless, PQLI parameter seems to be a good indicator for reduced visibility in fog but does not provide hint for the conditions outside of the clouds. To some extent, such information could be acquired from PQL. Unfortunately, it currently seems that absolute unification of these parameters (cloud liquid water content from radiation and microphysics) is difficult. The users of the visibility products (e.g. forecasters, aviation meteorologists) must be informed that the calculated fields are currently approximations to the real visibility, concerning both its quantity and qualitative distribution. Due to rather large uncertainty, even at very short forecast ranges, it could be recommended to implement this parameter in frame of an EPS system (e.g. LAEF).

Acknowledgements:
We would like to thank Ingrid Etchevers, Yann Seity (Meteo-France), Radmila Brožková and Ján Mašek (CHMI) and Neva Pristov (ARSO) for the discussions, information and materials, which helped the implementation of visibility at SHMÚ. We are also grateful to Claude Fischer and Ryad El Khatib for introducing the coding of visibility for the Training on code developments and validation at Meteo

France, which helped to understand the technical and coding aspects of implementation of this parameter in recent cycles of the model. We are also indebted to Oldřich Španiel (SHMÚ) for many ideas and for technical assistance.

References:

Achtemeier, G.L., 2008: Effects of Moisture Released during Forest Burning on Fog Formation and Implications for Visibility, *J. Appl. Meteor.* ,47, 1287-1296.

Dombrowski-Etchevers, I., Sanchez, I., Seity, Y., 2018: La visibilité : nouveau parametre issu des modeles de prévision météorologique. Presentation. Ateliers de Modélisation de l'Atmosphere, AMA, February 2018.

Gultepe, I., M. D. Muller, and Z. Boybeyi, 2006: A new visibility parameterization for warm fog applications in numerical weather prediction models. J. Appl. Meteor. Climatol., 45, 1469–1480.

Gultepe, I., Milbrandt, J. A., 2007: Microphysical observations and mesoscale model simulation of a warm fog case during FRAM project. Pure and Applied Geophysics, 164, 1161-1178.

Gultepe, I., J. Milbrandt, and Z. Binbin, 2010: Visibility Parameterization For Forecasting Model Applications, 5th International Conference on Fog, Fog Collection and Dew, Münster, Germany, 25–30 July 2010, FOGDEW2010-112

Kunkel, B. A., 1984: Parameterization of droplet terminal velocity and extinction coefficient in fog models. J. Climate Appl. Meteor., 23, 34–41.

Philip, Alexandre, 2016: *Apport d'une résolution verticale plus fine dans le calcul des tendances physiques pour la modélisation du brouillard dans le modèle AROME.* Thesis. Université de Toulouse, 122 pp.

Piriou, J.-M., Etchevers, I., Seity, Y., 2019: ARPEGE and AROME: recent developments and plans, ALADIN/HIRLAM workshop, Madrid, April 3, 2019

Sekula, P., 2018: Testing of new diagnostic fields: convective pack in cy43t2 and visibility in ALARO. ALADIN flat-rate stay report. Ljubljana 12.08.2018 – 8.09.2018

Stoelinga, M. T., and T. T. Warner, 1999: Nonhydrostatic,mesobetascalemodel simulations of cloud ceiling and visibility for an East Coast winter precipitation event. J. Appl. Meteor., 38, 385–404.